


 Cite this: *Chem. Commun.*, 2025, 61, 12187

 Received 9th June 2025,
 Accepted 4th July 2025

DOI: 10.1039/d5cc03251b

rsc.li/chemcomm

Achieving a dramatic blue colour stability in anthocyanins bearing acylated sugars in position 3',5'†

 Joana Oliveira,^a João T. S. Coimbra,^a Victor Freitas,^a Peiqing Yang,^{b,c} Nuno Basílio^b and Fernando Pina^b

A comparison of the thermodynamics and kinetics of two triacylated anthocyanins, pigment 1 from *Clitoria ternatea* (blue pea) and pigment 2 from *Ipomoea tricolor* (morning glory) reveals that, beyond the number of acylated units, the position of the sugar residues plays a crucial role in their stability.

Anthocyanins are the colorants conferring the different colour shades from red to blue of many flowers and fruits. Anthocyanins are constituted by a complex network of chemical species reversibly interconnected by proton transfer, hydration, tautomerization and *cis-trans* isomerization reactions, as reported in Scheme 1.¹

Simple anthocyanins are limited in their capacity to confer colour, exemplified in Fig. 1, for malvidin 3-*O*-glucoside. The red colour appears only at very acidic pH, the pink-magenta quinoidal base is a minor species and the blue anionic quinoidal base is unstable.¹

Nature overcomes this limitation, particularly in producing blue coloration, through the interaction of anthocyanins with metal ions or *via* intramolecular copigmentation involving acylated anthocyanins.^{2,3}

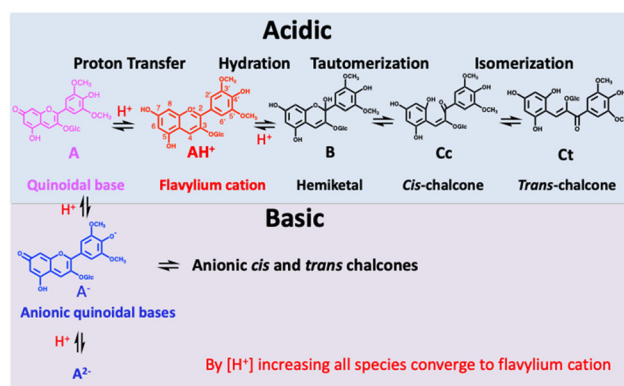
A previous study reported that the efficiency of intramolecular copigmentation in generating and stabilizing quinoidal bases increases with the number of acylated units (see Scheme S1, ESI†).⁴ However, the present work demonstrates that the number of acylated units alone does not determine stability; rather, the position of glycosylation sites

and their corresponding acylation patterns also play a critical role in enhancing the stability of the blue colour.

Polyacylated anthocyanins extracted from *Clitoria ternatea* have been reported to exhibit remarkable stability.⁵ To investigate the origin of this stability, the kinetics and thermodynamics of two triacylated anthocyanins, pigment 1 extracted from the *Clitoria ternatea* (Blue pea) (see Section S1 from the ESI†), and pigment 2 from *Ipomoea tricolor* (morning glory),⁴ Scheme 2, were compared.

The spectral variations of pigment 1 taken immediately after the addition of base to the flavylium cation (direct pH jump) are shown in Fig. S1 in the ESI.† Based on these absorption spectra, the respective titration curves were obtained as presented in Fig. 2. Fitting of Fig. 2 was obtained for the acidity constants reported in Table 1.

The stability of pigment 1 was monitored over two weeks, and Fig. 3 shows the time-dependent changes in the absorption, measured at the maximum wavelength, over a wide range of pH values. Except at pH values above 10.5, the absorption spectra recorded after 15 days showed only minor changes, indicating that the pH-dependent equilibrium between the



Scheme 1 Network of reversible chemical reactions involving anthocyanins and related pigments.

^a LAQV – REQUIMTE, Departamento de Química e Bioquímica, Faculdade de Ciências, Universidade do Porto, Rua do Campo Alegre, 687, 4169-007 Porto, Portugal. E-mail: jsoliveira@fc.up.pt

^b LAQV – REQUIMTE, Departamento de Química, Faculdade de Ciências e Tecnologia, Universidade Nova de Lisboa, 2829-516 Caparica, Portugal. E-mail: fp@fct.unl.pt

^c College of Food Science and Nutritional Engineering, Agricultural University, China

† Electronic supplementary information (ESI) available. See DOI: <https://doi.org/10.1039/d5cc03251b>



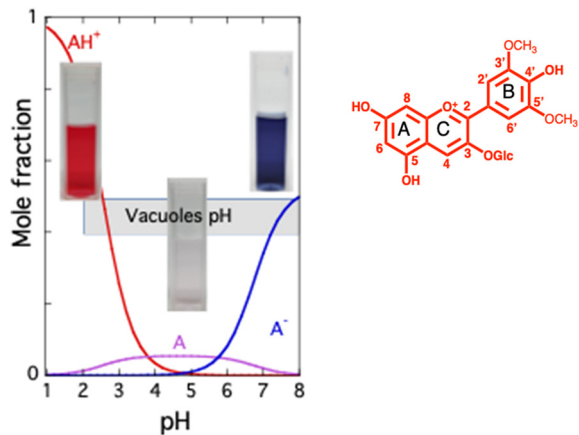


Fig. 1 Mole fraction distribution of the coloured species of malvidin 3-O-glucoside, AH⁺ and A, after 6 hours. The blue colour of A⁻ starts to fade during this time interval.

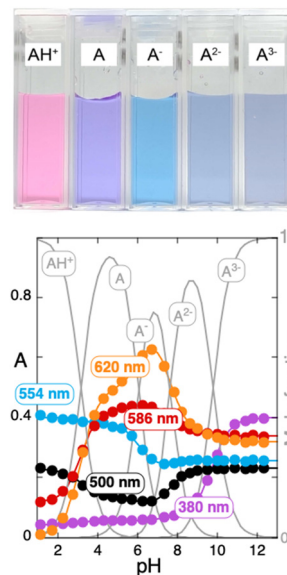
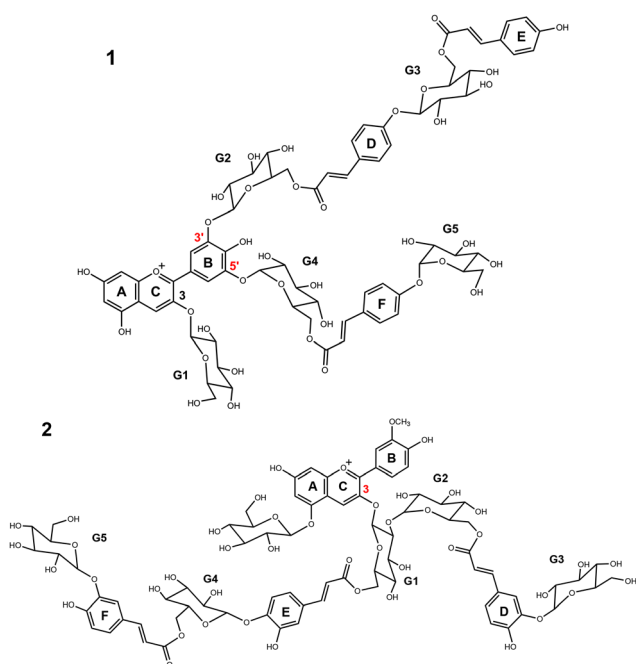


Fig. 2 Titration curves of pigment 1 immediately after a direct pH jump at five representative wavelengths.

Table 1 Acidity constants of pigments 1 and 2

Pigment	pK _{AH⁺/A}	pK _{A/A⁻}	pK _{A⁻/A²⁻}	pK _{A²⁻/A³⁻}
1	3.2	6.1	7.6	9.8
2 ^a	3.8	7.4	9.0	N/A

For pigment 2, $k_h = 0.01 \text{ s}^{-1}$ and $k_{-h} = 380 \text{ M}^{-1} \text{ s}^{-1}$.



Scheme 2 Structures of the two acylated anthocyanins bearing 3 acylated units. Pigment 1 was obtained from *Clitoria ternatea* and pigment 2 was obtained from *Ipomoea tricolor*.

flavylium cation and the respective quinoidal base forms remained largely stable over time.

Pigment 1 exhibits notable stability under acidic conditions, with only minimal degradation observed at higher pH values. Pigment 1 not only degrades at an extremely low rate but also does not undergo equilibration with the other species in the network presented in Scheme 1. This behaviour can be attributed to effective intramolecular copigmentation, which protects the chromophore by inhibiting the hydration reaction at the C-2 position. As a result, both progression toward the equilibrium state and degradation pathways are significantly suppressed.

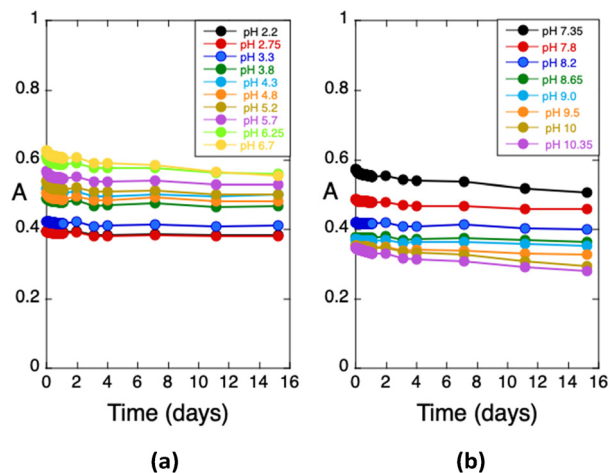


Fig. 3 Variation of the absorbance at maximum absorption wavelength as a function of pH for pigment 1; (a) acidic medium; (b) basic medium up to pH 10.35.

The stability of pigment 1 was compared with that of pigment 2, as both possess the same number of acylated units. In the case of pigment 2, a significant increase in the mole fraction of the quinoidal base is observed, along with enhanced stability of the blue anionic quinoidal base (Fig. 4), when compared to non-acylated anthocyanins like malvidin-3-O-glucoside. However, pigment 2 undergoes hydration relatively



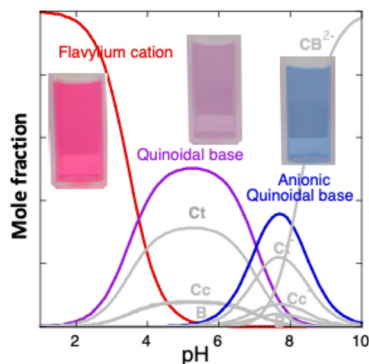


Fig. 4 Mole fraction distribution at the equilibrium of pigment 2. There is a huge increase in the mole fraction distribution of A and an increasing stability of A⁻ compared with Fig. 1. However, formation of the neutral, anionic and di-anionic species B, Ccⁿ⁻ Ctⁿ⁻ (n = 0,1,2) still occurs. CB²⁻ = Cc²⁻ + Ct²⁻.

fast, contrarily to pigment 1. The typical pH-dependent equilibrium seen in common anthocyanins is established (Table 1). This involves interconversion between the flavylium cation, quinoidal bases, hemiketal, and both *cis* and *trans*-chalcones, Fig. 4.‡

Given that both molecules contain the same number of acyl groups, but positioned differently within the structure, NOESY NMR structural elucidation combined with computational studies was employed to gain deeper insight into the conformations that pigment 1 and pigment 2 can adopt in solution. To this end, a conformational search using the CREST software was conducted to identify the conformer that best reproduced the observed long-range NOESY signals (Table S1, ESI†).^{6–11} Given that methanol was used as the solvent, the probability of intermolecular interactions was assumed to be low.¹² Consequently, the NOESY signals were primarily attributed to intramolecular interactions within the anthocyanin molecule.

To determine the most representative conformer of pigment 1, the goal was to minimize the sum of the interproton distances detected by NOESY (Table S1, ESI†). A similar procedure was applied to pigment 2, using NOESY data previously reported in the literature.⁷ The resulting conformers are shown in Fig. 5, with key NOESY distances highlighted. Both structures exhibit a highly stacked conformation, in agreement with earlier findings for pigment 2.⁷ However, the conformers in Fig. 5 reveal that pigment 1 adopts a more compact structure, characterized by stronger intramolecular stacking between the acylated rings and the flavylium chromophore. In contrast, pigment 2 exhibits a more open conformation, with a slightly higher solvent accessibility at the C-2 position.

Moreover, since nucleophilic water addition to the flavylium cation form of anthocyanins at position C-2 is a well-known process in aqueous solutions, leading to the formation of a colourless hemiketal,¹³ it was important to analyse the solvent exposure at this position. The degree of solvent accessibility at C-2 can influence the thermodynamics of this hydration reaction and, consequently, the equilibrium between the coloured and colourless forms. Comparative analysis of pigment 1 and

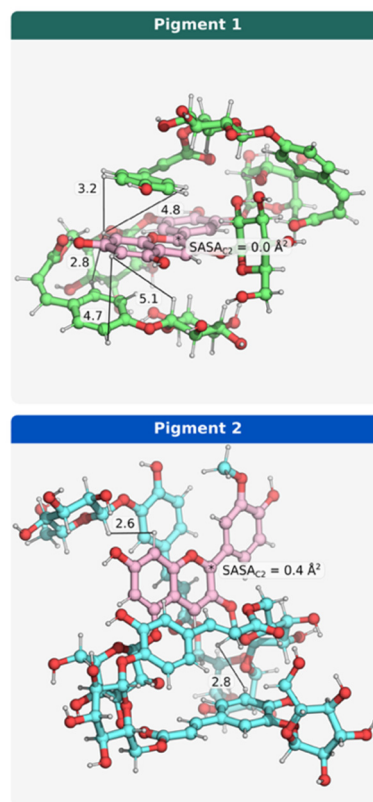


Fig. 5 Conformers that best minimized the sum of NMR-detected interproton distances (in Å) for pigment 1 and pigment 2. Anthocyanin structures are shown as ball-and-sticks, with key interproton distances highlighted. The flavylium cation backbone is presented in pink. The solvent accessible surface area at C-2 (*SASA_{C2}) is also given.

pigment 2 showed greater stabilization of the coloured⁴ forms in pigment 1, which correlated with a lower solvent-accessible surface area (SASA) at the C-2 position (SASA_{C2} = 0.0 Å²) compared to pigment 2 (SASA_{C2} = 0.4 Å²), as calculated from the conformers shown in Fig. 5. In the case of the non-acylated anthocyanin, malvidin-3-*O*-glucoside, the obtained SASA at C-2 was 3.5 Å². This value is consistent with the reported *k*_h and *k*_{-h} rate constants for this anthocyanin, in line with the expected parameters of reactivity of anthocyanins.

Taken together, these findings suggest that variations in molecular stacking and solvent accessibility at C-2 of the flavylium core are closely related to the experimentally observed differences in stability between the two pigments. Likewise, this folded structure can also confer protection against auto-oxidation reactions leading to degradation.

In summary, the number of acylated units is not the sole factor in extending the pH range and stability of the blue colour; the position of the acylated sugars within the anthocyanin structure is also critical. Acylated sugars located on the B-ring¹⁴ provide more effective protection against hydration compared to those attached to C-ring.

It has been proposed that blue pigmentation was among the last to emerge in Nature, and similarly in the Anthropocene.^{15,16} The present results raise the question of whether the less common



anthocyanins bearing acylated groups at positions 3' and 5',¹⁷ may represent a more advanced evolutionary stage in the stabilization of the blue colour in plants.

This work received financial support from the PT national funds (FCT/MCTES, Fundação para a Ciência e Tecnologia and Ministério da Ciência, Tecnologia e Ensino Superior) through the project UID/50006 - Laboratório Associado para a Química Verde - Tecnologias e Processos Limpos. J. O. would like to thank FCT for her research contract (2022.00042.CEECIND/CP1724/CT0017). All authors defined the structure of this communication and contributed to the discussion and interpretation of the experimental results. J. O. and V. F. performed the extraction, purification, and structural characterization of pigment 1. P. Y. and N. B. conducted the physical-chemical studies. F. P. wrote the first draft and supervised all the work with J. O. J. T. S. C. performed, analyzed, and reported the in silico experiments. All authors revised the manuscript.

Conflicts of interest

There are no conflicts to declare.

Data availability

The datasets and software tools employed in this study are publicly accessible. CREST (version 3.0), a program for automated exploration of low-energy molecular chemical space, is available at <https://crest-lab.github.io/crest-docs/>. xTB (version 6.7.1), a semiempirical extended tight-binding program package, can be assessed at <https://xtb-docs.readthedocs.io/en/latest/>. Open-Source PyMOL (version 2.5.0), utilized for molecular visualization and image rendering, is obtainable from <https://github.com/schrodinger/pymol-open-source>. The commercial PyMOL product with maintenance and support is available from <https://pymol.org>. GaussView (version 6), the graphical interface used with Gaussian, is a licensed software available for purchase at <https://Gaussian.com/pricing>. Open Babel (version 3.1.1), a free, open-source version of the Babel chemistry file translation program, is available at <https://openbabel.org/>. All software tools mentioned are either open-source or commercially available, as specified. For any datasets generated during this study, please refer to the ESI† accompanying this manuscript. If further information is required, the corresponding author can be contacted *via* the provided institutional email address.

Notes and references

‡ Anionic hemiketal is unstable.

- 1 L. Cruz, N. B. N. Mateus, V. de Freitas and F. Pina, Natural and Synthetic Flavylum-Based Dyes: The Chemistry Behind the Color, *Chem. Rev.*, 2022, **122**, 1416–1481.
- 2 P. Trouillas, J. C. Sancho-García, V. De Freitas, J. Gierschner, M. Otyepka and O. Dangles, Stabilizing and modulating color by copigmentation: insights from theory and experiment, *Chem. Rev.*, 2016, **116**(9), 4937–4982.
- 3 K. Yoshida, M. Mori and T. Kondo, Blue flower color development by anthocyanins: from chemical structure to cell physiology, *Nat. Prod. Rep.*, 2009, **26**(7), 884–915.
- 4 J. Mendoza, N. Basilio, F. Pina, T. Kondo and K. Yoshida, Rationalizing the Color in Heavenly Blue Anthocyanin: A Complete Kinetic and Thermodynamic Study, *J. Phys. Chem. B*, 2018, **122**(19), 4982–4992.
- 5 T. Kondo, M. Ueda and T. Goto, Structure of ternatin-b1, a pentaacylated anthocyanin substituted on the b-ring asymmetrically with 2 long chains, *Tetrahedron*, 1990, **46**(13–14), 4749–4756.
- 6 C. Bannwarth, S. Ehlert and S. Grimme, GFN2-xTB—An Accurate and Broadly Parametrized Self-Consistent Tight-Binding Quantum Chemical Method with Multipole Electrostatics and Density-Dependent Dispersion Contributions, *J. Chem. Theory Comput.*, 2019, **15**(3), 1652–1671.
- 7 T. Goto and T. Kondo, Structure and Molecular Stacking of Anthocyanins—Flower Color Variation, *Angew. Chem., Int. Ed. Engl.*, 1991, **30**(1), 17–33.
- 8 N. M. O'Boyle, M. Banck, C. A. James, C. Morley, T. Vandermeersch and G. R. Hutchison, Open Babel: An open chemical toolbox, *J. Cheminf.*, 2011, **3**(1), 33.
- 9 P. Pracht, F. Bohle and S. Grimme, Automated exploration of the low-energy chemical space with fast quantum chemical methods, *Phys. Chem. Chem. Phys.*, 2020, **22**(14), 7169–7192.
- 10 P. Pracht, S. Grimme, C. Bannwarth, F. Bohle, S. Ehlert, G. Feldmann, J. Gorges, M. Müller, T. Neudecker, C. Plett, S. Spicher, P. Steinbach, P. A. Wesolowski and F. Zeller, CREST—A program for the exploration of low-energy molecular chemical space, *J. Chem. Phys.*, 2024, **160**, 11.
- 11 S. Spicher and S. Grimme, Robust Atomistic Modeling of Materials, Organometallic, and Biochemical Systems, *Angew. Chem., Int. Ed.*, 2020, **59**(36), 15665–15673.
- 12 R. Brouillard and O. Dangles, Anthocyanin molecular interactions: the first step in the formation of new pigments during wine aging?, *Food Chem.*, 1994, **51**(4), 365–371.
- 13 O. Dangles and J. A. Fenger, The Chemical Reactivity of Anthocyanins and Its Consequences in Food Science and Nutrition, *Molecules*, 2018, **23**, 8.
- 14 K. Kazuma, N. Noda and M. Suzuki, Flavonoid composition related to petal color in different lines of *Clitoria ternatea*, *Phytochemistry*, 2003, **64**(6), 1133–1139.
- 15 F. Pina, N. Basilio, A. J. Parola, M. J. Melo, J. Oliveira and V. de Freitas, The Triumph of the blue in nature and in Anthropocene, *Dyes Pigm.*, 2023, **210**, 110925.
- 16 O. R. Gottlieb, Blue Flower Pigmentation and Evolutionary Advancement, in *Micromolecular Evolution, Systematics and Ecology: An Essay into a Novel Botanical Discipline*, ed. O. R. Gottlieb, Springer Berlin Heidelberg: Berlin, Heidelberg, 1982, pp. 142–148.
- 17 O. M. M. Andersen, *Flavonoids: Chemistry, Biochemistry and Applications*, Taylor & Francis, USA, 2006.

